International Journal of Scientific Engineering and Science
Volume 10, Issue 4, pp. 5-11, 2026. ISSN (Online): 2456-7361

Radiological Risk Parameters Due to Gamma Radiation Emitted by Natural Radionuclides (^{238}U, ^{232}Th, and ^{40}K) in the Soil of Nosy-Be, Madagascar

DJAOVAGNONO Houssen Claude[1], DONNE Zafizara[1], RASOLONIRINA Martin[2], SOLONJARA Asivelo Fanantenansoa[2], KALL Briant[1]
[1]Department of Nuclear Metrology and Environment, Faculty of Science, University of Antsiranana, Madagascar
[2]Department of Nuclear Techniques and Analysis, National Institute of Sciences and Nuclear Techniques, Madagascar

Abstract*—Following the geochemical characterization and mapping of natural soil radioactivity in Nosy-Be (Djaovagnono et al., 2025), this study evaluates the dosimetric impacts and associated radiological risks for the local population and tourists. Based on the specific activities of ^{238}U (33 Bq·kg^{-1}), ^{232}Th (39 Bq·kg^{-1}), and ^{40}K (138 Bq·kg^{-1}) measured in 30 soil samples, we calculated the main risk indicators. The average radium equivalent activity is 99 ± 25 Bq·kg^{-1}, well below the threshold of 370 Bq·kg^{-1} for building materials. The absorbed dose rate in the air ranges from 27 to 94 nGy·h^{-1}, with an average of 44 ± 12 nGy·h^{-1}, which is lower than the global average of 59 nGy·h^{-1}. The average external annual effective dose for the population is estimated at 0.054 mSv·y^{-1} (for 20% outdoors) and 0.136 mSv·y^{-1} (for 50% outdoors), which are fractions of the 1 mSv·y^{-1} limit recommended for the public. The analysis confirms that even the radiological "hotspots" identified in our previous study, linked to the island's recent volcanic geology, do not present an acute health risk. However, the lifetime cancer risk for farmers (50% outdoors) slightly exceeds the global average. In conclusion, this dosimetric evaluation confirms that the natural radioactivity levels of Nosy-Be's soils are generally safe for human health, providing a solid scientific basis for radiation protection and land-use planning.*

Keywords*—Natural Radioactivity, Radium equivalent, Absorbed dose, Annual effective dose, Excess lifetime cancer risk.*

I. Introduction

The evaluation of human exposure to ionizing radiation of natural origin is an essential component of radiation protection and public health. The primary source of external exposure comes from primordial radionuclides present in the Earth's crust, notably those in the decay chains of uranium-238 (^{238}U) and thorium-232 (^{232}Th), as well as potassium-40 (^{40}K) (UNSCEAR, 2000). The concentration of these elements in soils and rocks is highly heterogeneous, being directly controlled by local geology, weathering processes, and, in some cases, anthropogenic activities (Namq *et al.,* 2025; Akuo-ko *et al.,* 2025).

Monitoring these radioactivity levels is essential for assessing long-term health risks, such as cancer development, especially since exposure varies considerably depending on lifestyles and urban or rural environments (Houndetoungan *et al.,* 2025; Mvelase, 2026). In Madagascar, geological diversity has led to several recent studies aimed at evaluating radiological risks in different districts. Moderate to high levels have thus been documented in Ambilobe (Stolerie *et al.,* 2022), Antalaha (Ngoko *et al.,* 2025), Antsiranana II with its volcanic soils (Tsilailay *et al.,* 2026), and in the Ambanja region, where notable radiological anomalies were identified (Rahelivao *et al.,* 2023).

In a previous study (Djaovagnono *et al.,* 2025), we performed the first geochemical characterization and mapped the spatial distribution of these radionuclides in the volcanic soils of Nosy-Be Island. This initial study revealed moderate natural radioactivity, with average specific activities of 33 ± 8 Bq·kg^{-1} for ^{238}U, 39 ± 9 Bq·kg^{-1} for ^{232}Th, and 138 ± 79 Bq·kg^{-1} for ^{40}K. The main contribution was highlighting a marked spatial heterogeneity, dictated by a geo-pedological duality: a western region derived from recent volcanism presenting higher concentrations, and an eastern region dominated by older formations and deeply weathered, leached ferralitic soils, particularly depleted in ^{40}K.

However, the question of direct health consequences had not been addressed until now. The present study is therefore the logical and indispensable continuation of this work. The objective of this study is to translate the specific activities of these natural radionuclides into concrete radiological risk indicators: radium equivalent activity (Ra_{eq}), absorbed gamma dose rate in air (*AGDR*), annual effective dose (*AEDR*) under different occupancy scenarios, and excess lifetime cancer risk (*ELCR*). These results will determine whether exposure to ambient radiation in Nosy-Be poses a danger to its permanent residents, particularly farmers and tourists, thereby providing a clear conclusion regarding the island's radiological safety.

II. Materials and Methods

2.1. Description of the Study Site

The study was conducted on the island of Nosy-Be, which covers an area of approximately 320 km² of the northwest coast of Madagascar, in the DIANA region. The island is located between latitudes 13°09′45.13" and 13°30′17.93" South and longitudes 48°07′31.92" and 48°24′21.18" East (Fig. 1). Nosy-Be presents a unique geo-climatic context. Its geology is characterized by a mosaic of Cenozoic volcanic formations resting on a Mesozoic sedimentary basement. The region is subject to a humid tropical climate, favoring intense chemical weathering of parent materials, which directly influences soil formation and the retention or leaching of radionuclides (Djaovagnono *et al.,* 2025).

International Journal of Scientific Engineering and Science
Volume 10, Issue 4, pp. 5-11, 2026. ISSN (Online): 2456-7361

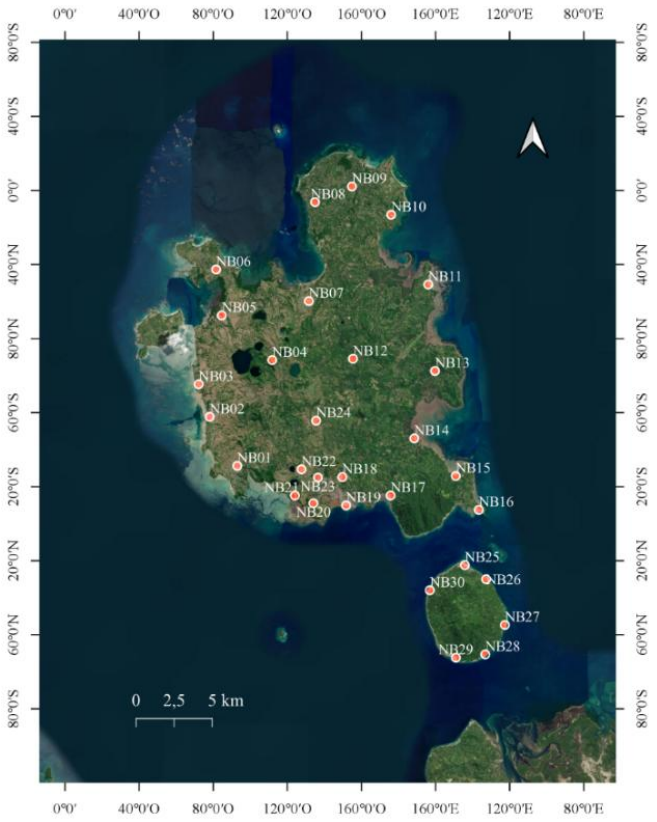

Fig. 1. Location of the study Site and sampling points

2.2. Sampling Strategy and laboratory work

The sampling strategy covered the different geo-pedological formations of the island in a representative manner. In total, 30 soil samples were taken at a depth of about 30 cm. The geographic coordinates (Latitude and Longitude) of each sampling point are listed in Table I.

TABLE I. GPS coordinates of the sampling points

Sample ID	GPS Coordination	
	Latitude (N)	Longitude (E)
NB01	13°23'00.88"S	48°12'32.71"E
NB02	13°21'16.96"S	48°11'32.59"E
NB03	13°20'07.61"S	48°11'08.86"E
NB04	13°19'16.23"S	48°13'49.09"E
NB05	13°17'41.38"S	48°11'58.99"E
NB06	13°16'03.83"S	48°11'46.68"E
NB07	13°17'10.87"S	48°15'09.06"E
NB08	13°13'40.58"S	48°15'22.59"E
NB09	13°13'07.20"S	48°16'43.08"E
NB10	13°14'07.47"S	48°18'08.84"E
NB11	13°16'35.65"S	48°19'29.49"E
NB12	13°19'13.56"S	48°16'45.28"E
NB13	13°19'39.27"S	48°19'44.28"E
NB14	13°22'02.59"S	48°18'59.23"E
NB15	13°23'22.44"S	48°20'29.59"E
NB16	13°24'34.38"S	48°21'19.77"E
NB17	13°24'03.86"S	48°18'07.53"E
NB18	13°23'24.64"S	48°16'22.27"E
NB19	13°24'24.96"S	48°16'30.32"E
NB20	13°24'20.26"S	48°15'19.17"E
NB21	13°24'03.93"S	48°14'38.67"E
NB22	13°23'08.44"S	48°14'53.07"E
NB23	13°23'25.90"S	48°15'28.80"E
NB24	13°21'24.89"S	48°15'25.07"E
NB25	13°26'31.79"S	48°20'49.39"E
NB26	13°27'01.76"S	48°21'35.57"E
NB27	13°28'38.74"S	48°22'16.80"E
NB28	13°29'41.33"S	48°21'33.92"E
NB29	13°29'48.19"S	48°20'29.75"E
NB30	13°27'25.09"S	48°19'32.92"E

The samples were dried, crushed, sieved, and sealed for at least three weeks to reach secular equilibrium. Measurements were performed by gamma spectrometry using a NaI(Tl) scintillation detector. Table II summarizes the measured specific activities, indicating averages of 33 Bq·kg^{-1} for ^{238}U, 39 Bq·kg^{-1} for ^{232}Th, and 138 Bq·kg^{-1} for ^{40}K (Djaovagnono *et al.,* 2025).

TABLE II. Specific activities of natural radionuclides in the volcanic soil of Nosy-Be

Sample ID	Specific activity (Bq.kg^{-1})		
	^{238}U	^{232}Th	^{40}K
NB01	26 ± 2	30 ± 5	128 ± 6
NB02	33 ± 2	41 ± 4	166 ± 6
NB03	40 ± 2	46 ± 4	106 ± 5
NB04	27 ± 2	47 ± 4	122 ± 6
NB05	41 ± 3	44 ± 8	175 ± 11
NB06	31 ± 2	34 ± 5	178 ± 7
NB07	33 ± 2	34 ± 4	134 ± 6
NB08	39 ± 2	39 ± 4	51 ± 4
NB09	34 ± 1	32 ± 3	194 ± 6
NB10	35 ± 1	44 ± 3	146 ± 5
NB11	33 ± 2	30 ± 5	138 ± 6
NB12	26 ± 1	36 ± 3	52 ± 3
NB13	43 ± 1	51 ± 4	214 ± 7
NB14	42 ± 2	40 ± 4	128 ± 6
NB15	34 ± 2	37 ± 4	157 ± 6
NB16	24 ± 1	22 ± 3	73 ± 3
NB17	32 ± 2	42 ± 4	64 ± 4
NB18	29 ± 2	38 ± 5	100 ± 6
NB19	35 ± 2	37 ± 5	130 ± 7
NB20	27 ± 2	34 ± 6	185 ± 8
NB21	33 ± 2	44 ± 5	129 ± 6
NB22	25 ± 2	36 ± 5	138 ± 7
NB23	32 ± 2	33 ± 5	109 ± 6
NB24	68 ± 3	71 ± 7	480 ± 16
NB25	25 ± 1	27 ± 3	68 ± 4
NB26	24 ± 1	30 ± 3	92± 4
NB27	28 ± 1	35 ± 3	104 ± 5
NB28	28 ± 2	51 ± 4	99 ± 5
NB29	32 ± 2	42 ± 4	64 ± 4
NB30	28 ± 2	34 ± 5	205 ± 8
Mean ± σ	**33 ± 8**	**39 ± 9**	**138 ± 79**

2.3. Determination of Radiological Risk Parameters

2.3.1. Radium Equivalent Activity (Ra_{eq})

To assess the overall radiological hazard, particularly if the soils are used as building materials, the radium equivalent activity was calculated. It normalizes the activity of ^{238}U, ^{232}Th, and ^{40}K into a single value corresponding to the activity of ^{226}Ra that would produce the same gamma dose rate. The formula used was initially proposed by (Beretka and Mathew, 1985) and is widely applied in recent radiological studies in Madagascar (Stolerie *et al.,* 2022; Ngoko *et al.,* 2025):

$$Ra_{eq} = A_U + 1.43 \times A_{Th} + 0.077 \times A_K \quad (1)$$

Where A_U, A_{Th}, and A_K are the specific activities (in Bq·kg^{-1}). A material is considered safe for construction if its

International Journal of Scientific Engineering and Science
Volume 10, Issue 4, pp. 5-11, 2026. ISSN (Online): 2456-7361

radium equivalent value is below the recommended limit of 370 Bq·kg⁻¹ (UNSCEAR, 2000).

2.3.2. Absorbed Gamma Dose Rate in Air (AGDR)

The absorbed dose rate at 1 meter above the ground was calculated based on the assumption that all decay products of uranium and thorium are in radioactive equilibrium with their precursors. This calculation uses the dose-to-activity conversion factors established by (UNSCEAR, 2000) and frequently used in the literature (Tzortzis *et al.,* 2003; El-Bahi *et al.,* 2017):

$$AGDR = 0.462 \times A_U + 0.604 \times A_{Th} + 0.0417 \times A_K \quad (2)$$

Where A_U, A_{Th}, and A_K are the respective specific activities (in Bq·kg⁻¹).

2.3.3. *Annual Effective Dose Rate (AEDR)*

To estimate the long-term biological impact, the absorbed dose in the air is converted into an external annual effective dose (*AEDR*). This calculation incorporates a conversion coefficient of 0.7 Sv·Gy⁻¹ to transition from the absorbed dose to the effective dose received by an adult, along with a total annual exposure time of 8766 hours (UNSCEAR, 2000).

To reflect local realities and population habits, two occupancy factor (*OF*) scenarios were modeled (Stolerie *et al.,* 2022; Ngoko *et al.,* 2025):

(1). **20% outdoors** (international standard, *OF* = 0.2), corresponding to urban populations spending the majority of their time indoors (UNSCEAR, 2000).

(2). **50% outdoors** (*OF* = 0.5), corresponding to the rural and agricultural Malagasy population who spend about half of their time (from 6 a.m. to 6 p.m.) in the fields (Rahelivao *et al.,* 2023).

The applied formula is as follows:

$$AEDR = AGDR \times T \times Q \times OF \times 10^{-6} \quad (3)$$

The acceptable annual effective dose limit for the general public is set at 1 mSv·y⁻¹ (UNSCEAR, 2000; ICRP, 2007).

2.3.4. *Excess Lifetime Cancer Risk (ELCR)*

This parameter estimates the stochastic probability that an individual will develop cancer over their lifetime due to continuous exposure to ambient gamma radiation emitted by the soil. It is calculated using the following relationship (Ngoko *et al.,* 2025; Tsilailay *et al.,* 2026):

$$ELCR = AEDR \times DL \times RF \quad (4)$$

Where *DL* is the average life expectancy (set at 70 years according to global standards to allow for direct international comparison) and *RF* is the fatal cancer risk factor, estimated at 0.055 Sv⁻¹ for the general public (UNSCEAR, 2000; ICRP, 2007).

III. Results and Discussion

Table III below summarizes the various values of radium equivalent activities and absorbed dose rates in the air at 1 m from the ground estimated in the soils of the Nosy-Be district.

3.1. Radium Equivalent Activity (Ra_{eq})

Table III presents the Ra_{eq} values, which range between (61 ± 4) and (206 ± 11) Bq·kg⁻¹, with an average of (99 ± 25) Bq·kg⁻¹. All 30 sampled sites exhibit values well below the global safety threshold of 370 Bq·kg⁻¹. This signifies that the use of local soils for brick making or construction poses no radiological danger.

TABLE III. Radium equivalent activity and absorbed dose in the air

Sample ID	Ra_{eq} (Bq.kg⁻¹)	*AGDR* (nGy.h⁻¹)
NB01	79 ± 7	35 ± 3
NB02	104 ± 6	47 ± 3
NB03	114 ± 6	51 ± 3
NB04	104 ± 6	46 ± 3
NB05	117 ± 12	53 ± 5
NB06	93 ± 7	42 ± 3
NB07	92 ± 6	41 ± 3
NB08	99 ± 6	44 ± 3
NB09	95 ± 4	43 ± 2
NB10	109 ± 4	49 ± 2
NB11	87 ± 7	39 ± 3
NB12	81 ± 4	36 ± 2
NB13	132 ± 6	60 ± 2
NB14	109 ± 6	49 ± 3
NB15	99 ± 6	45 ± 3
NB16	61 ± 4	27 ± 2
NB17	97 ± 6	43 ± 3
NB18	91 ± 7	41 ± 3
NB19	98 ± 7	44 ± 3
NB20	90 ± 9	41 ± 4
NB21	106 ± 7	47 ± 3
NB22	87 ± 7	39 ± 3
NB23	88 ± 7	39 ± 3
NB24	206 ± 11	94 ± 4
NB25	69 ± 4	31 ± 2
NB26	74 ± 4	33 ± 2
NB27	86 ± 4	38 ± 2
NB28	109 ± 6	48 ± 3
NB29	97 ± 6	43 ± 3
NB30	92 ± 7	42 ± 3
Min - Max	**61 - 206**	**27 - 94**
Mean ± σ	**99 ± 25**	**44 ± 12**
Reference value	**370**	**59**

Fig. 2 illustrates the spatial distribution of this parameter. It is clearly observable that the highest values (the "hotspots" in red) are concentrated in the western part of the island. This distribution validates our earlier geological observations: young soils derived from recent (Pleistocene) volcanism retain more radionuclides than the highly leached ferralitic soils of the east coast.

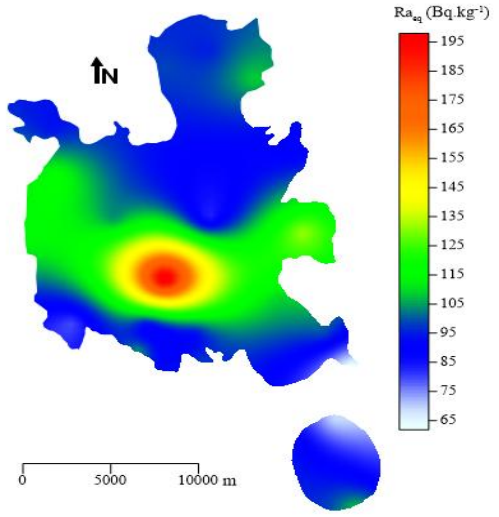

Fig. 2. Spatial distribution of radium equivalent activities

International Journal of Scientific Engineering and Science
Volume 10, Issue 4, pp. 5-11, 2026. ISSN (Online): 2456-7361

3.2. Absorbed dose rate in air at 1 m from the ground (AGDR)

The absorbed dose rate (*AGDR*) varies from (27 ± 2) to (94 ± 4) nGy·h⁻¹, with an average of 44 ± 12 nGy·h⁻¹ (Table III). This average is notably lower than the established global average of 59 nGy·h⁻¹. The spatial mapping of the AGDR (Fig. 3) logically superimposes onto that of Ra_{eq}, pointing to the same localized anomalies in the west. Although sample NB24 reaches 94 nGy·h⁻¹, exceeding the global average, it remains an isolated point linked to a specific rocky outcrop and does not represent a generalized ambient hazard.

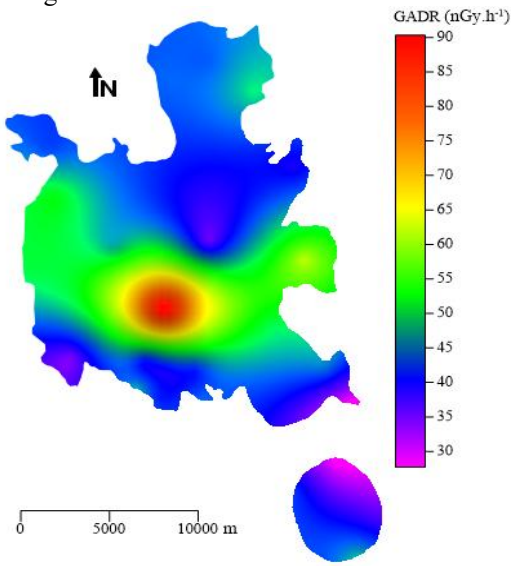

Fig. 3. Spatial distribution of absorbed doses in air at 1 m from the ground

3.3. Annual effective doses (AEDR) at 20% and 50%

Table IV highlights the importance of lifestyle in risk assessment.

TABLE IV. Annual effective doses estimated at 20% and 50% outdoors

Sample ID	*AEDR*, 20% outdoors (mSv.y⁻¹)	*AEDR*, 50% outdoors (mSv.y⁻¹)
NB01	0.044 ± 0.004	0.109 ± 0.010
NB02	0.058 ± 0.003	0.144 ± 0.008
NB03	0.062 ± 0.003	0.156 ± 0.008
NB04	0.056 ± 0.003	0.141 ± 0.008
NB05	0.065 ± 0.006	0.162 ± 0.015
NB06	0.052 ± 0.004	0.130 ± 0.010
NB07	0.051 ± 0.003	0.127 ± 0.008
NB08	0.054 ± 0.003	0.134 ± 0.008
NB09	0.053 ± 0.002	0.132 ± 0.006
NB10	0.06 ± 0.002	0.150 ± 0.006
NB11	0.048 ± 0.004	0.120 ± 0.010
NB12	0.044 ± 0.002	0.110 ± 0.006
NB13	0.073 ± 0.003	0.183 ± 0.008
NB14	0.06 ± 0.003	0.150 ± 0.008
NB15	0.055 ± 0.003	0.137 ± 0.008
NB16	0.034 ± 0.002	0.084 ± 0.006
NB17	0.053 ± 0.003	0.131 ± 0.008
NB18	0.05 ± 0.004	0.124 ± 0.010
NB19	0.054 ± 0.004	0.135 ± 0.010
NB20	0.05 ± 0.005	0.125 ± 0.012
NB21	0.058 ± 0.004	0.145 ± 0.010
NB22	0.048 ± 0.004	0.120 ± 0.010
NB23	0.048 ± 0.004	0.120 ± 0.010
NB24	0.116 ± 0.006	0.289 ± 0.014
NB25	0.038 ± 0.002	0.094 ± 0.006
NB26	0.041 ± 0.002	0.101 ± 0.006
NB27	0.047 ± 0.002	0.118 ± 0.006
NB28	0.059 ± 0.003	0.147 ± 0.008
NB29	0.053 ± 0.003	0.131 ± 0.008
NB30	0.052 ± 0.004	0.129 ± 0.010
Min - Max	**0.034 - 0.116**	**0.084 - 0.289**
Mean ± σ	**0.054 ± 0.014**	**0.136 ± 0.035**
Reference value	**1**	**1**

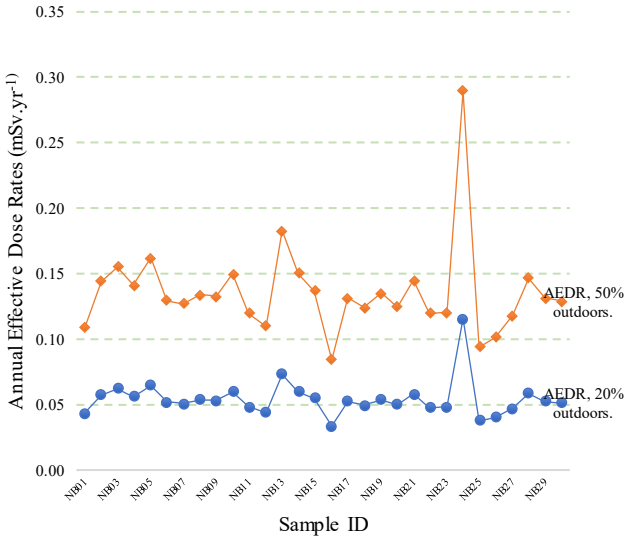

Fig. 4. Variation of Annual Effective Dose Rates for 20% and 50% outdoors

For a population spending 20% of their time outdoors, the average effective dose is very low: 0.054 mSv·y⁻¹ (ranging from 0.034 to 0.116 mSv·y⁻¹). For farmers spending 50% of their time outdoors, this average dose rises to 0.136 mSv·y⁻¹ (ranging from 0.084 to 0.289 mSv·y⁻¹). Indeed, Fig. 4 allows us to visualize this systemic gap between the two exposure profiles. The major takeaway here is that, even in the worst-case scenarios (a farmer working on the most radioactive soil on the island), the maximum received dose (0.289 mSv·y⁻¹) remains well below the 1 mSv·y⁻¹ limit recommended by the International Commission on Radiological Protection (ICRP). Therefore, external exposure does not generate any acute health risk.

3.4. Excess lifetime cancer risk (ELCR) estimated at 20% and 50%

Table V translates the annual effective doses into the probability of developing cancer over a 70-year lifespan. For the 20% outdoor scenario, the average *ELCR* is 0.21×10^{-3}, a reassuring value as it is below the global average of 0.29×10^{-3}. However, for the agricultural scenario (50% outdoors), the average increases to 0.52×10^{-3} (ranging from 0.32 to 1.11×10^{-3}).

Figure 5 illustrates the statistical distribution of the Excess Lifetime Cancer Risk (*ELCR*) calculated for two exposure scenarios (20% and 50% of time spent outdoors) using boxplots. This graphical representation serves as a powerful visual test to analyze dispersion, central tendency, interquartile range, and data skewness relative to the global reference value set at 0.29×10^{-3}.

International Journal of Scientific Engineering and Science
Volume 10, Issue 4, pp. 5-11, 2026. ISSN (Online): 2456-7361

Table V. Excess lifetime cancer risk estimated at 20% and 50% outdoors

Sample ID	*ELCR* [20% outdoors] ($\times 10^{-3}$)	*ELCR* [50% outdoors] ($\times 10^{-3}$)
NB01	0.17 ± 0.01	0.42 ± 0.04
NB02	0.22 ± 0.01	0.55 ± 0.03
NB03	0.24 ± 0.01	0.60 ± 0.03
NB04	0.22 ± 0.01	0.54 ± 0.03
NB05	0.25 ± 0.02	0.62 ± 0.06
NB06	0.20 ± 0.01	0.50 ± 0.04
NB07	0.20 ± 0.01	0.49 ± 0.03
NB08	0.21 ± 0.01	0.52 ± 0.03
NB09	0.20 ± 0.01	0.51 ± 0.02
NB10	0.23 ± 0.01	0.58 ± 0.02
NB11	0.18 ± 0.01	0.46 ± 0.04
NB12	0.17 ± 0.01	0.42 ± 0.02
NB13	0.28 ± 0.01	0.70 ± 0.03
NB14	0.23 ± 0.01	0.58 ± 0.03
NB15	0.21 ± 0.01	0.53 ± 0.03
NB16	0.13 ± 0.01	0.32 ± 0.02
NB17	0.20 ± 0.01	0.51 ± 0.03
NB18	0.19 ± 0.01	0.48 ± 0.04
NB19	0.21 ± 0.01	0.52 ± 0.04
NB20	0.19 ± 0.02	0.48 ± 0.04
NB21	0.22 ± 0.01	0.56 ± 0.04
NB22	0.18 ± 0.01	0.46 ± 0.04
NB23	0.19 ± 0.01	0.46 ± 0.04
NB24	0.45 ± 0.02	1.11 ± 0.05
NB25	0.15 ± 0.01	0.36 ± 0.02
NB26	0.16 ± 0.01	0.39 ± 0.02
NB27	0.18 ± 0.01	0.45 ± 0.02
NB28	0.23 ± 0.01	0.57 ± 0.03
NB29	0.20 ± 0.01	0.51 ± 0.03
NB30	0.20 ± 0.02	0.50 ± 0.04
Min - Max	**0.13 - 0.45**	**0.32 - 1.11**
Mean ± σ	**0.21 ± 0.05**	**0.52 ± 0.14**
Reference value	**0.29**	**0.29**

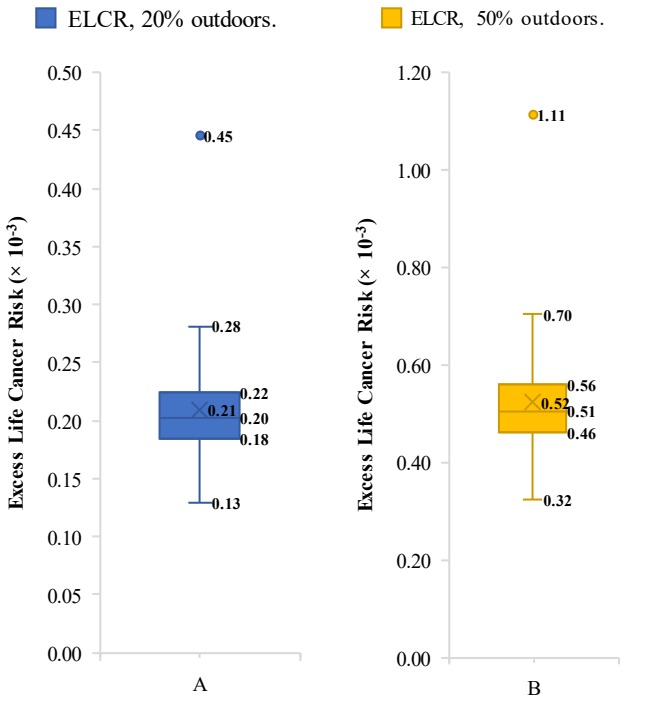

Fig. 5. Representation of excess lifetime cancer risks estimated at 20% and 50% outdoors using boxplots

The analysis of the quartiles yields the following statistical conclusions:

(1). For the urban/standard scenario (20% outdoors): The boxplot shows that almost the entirety of the distribution lies within a safe zone. The first quartile (Q1), the median (50th percentile, located at 0.20×10^{-3}), and the third quartile (Q3) are found distinctly below the global reference line of 0.29×10^{-3}. The interquartile range (the difference between Q1 and Q3, representing the central 50% of the sample's values) is narrow, indicating low dispersion in radioactivity for the majority of the sites. This means that for more than 75% of the points measured in Nosy-Be, the cancer risk remains statistically lower than the global average. Only the tip of the upper whisker (maximum value at 0.45×10^{-3}) crosses the reference line, which corresponds to a few geographically isolated outliers.

(2). For the rural/agricultural scenario (50% outdoors): The visual test reveals a spectacular shift of the statistical distribution toward higher risk values. In this scenario, the lower whisker (the absolute minimum value of the sample, 0.32×10^{-3}) already exceeds the global reference line of 0.29×10^{-3}. Consequently, the entire interquartile box (from Q1 to Q3) and the median (at 0.51×10^{-3}) are situated well above the reference threshold. Statistically, this demonstrates that 100% of the sampled sites present a higher cancer risk than the global average if the individual adopts an agricultural lifestyle (spending half of their time in direct contact with the outdoor soil).

(3). Distribution Skewness: For both scenarios, observation of the boxplots reveals a skewed distribution. The upper whisker is notably longer than the lower one, and the arithmetic mean is consistently "pulled" above the median. This morphology characterizes an asymmetric distribution stretched to the right (positive skewness). From a geostatistical viewpoint, this confirms that there is no perfect homogeneity of soils on the island: a vast majority of soils present moderate ambient radioactivity, but a restricted group of sites originating from recent volcanism acts as anomalies stretching the distribution towards extreme values (respective maximums of 0.45×10^{-3} and 1.11×10^{-3}).

The total lack of overlap between the 20% scenario box (mostly below the limit) and the 50% scenario box (entirely above the limit) proves in a statistically significant manner that the critical parameter governing radiological risk in Nosy-Be is not the intensity of the geological radioactivity itself, but rather the occupancy factor (the outdoor exposure time linked to population lifestyle).

The results obtained in Nosy-Be take on full meaning when placed in perspective with other recently studied districts in Madagascar (Table VI).

In Nosy-Be, the effective dose (*AEDR* for 50%) of 0.14 $mSv.y^{-1}$ and the cancer risk (*ELCR*) of 0.52×10^{-3} are very similar to the values reported for the districts of Ambilobe (0.18

mSv.y^{-1}; *ELCR* = 0.50×10^{-3}) (Stolerie *et al.,* 2022) and Antalaha (0.18 mSv.y^{-1}; *ELCR* = 0.53×10^{-3}) (Ngoko *et al.,* 2025). These three regions share relatively calm natural radioactivity profiles, dictated by sedimentary basins or standard volcanic rocks.

TABLE VI. Comparison of radiological hazard indices with other districts

District	Ra_{eq} (Bq.kg^{-1})	*AGDR* (nGy.h^{-1})	*AEDR* (mSv.y^{-1})	*ELCR* (x10^{-3})
Nosy Be (Present study)	99.00	44.00	0.05 (20%) 0.14 (50%)	0.21 (20%) 0.52 (50%)
Ambanja (Rahelivao *et al.,* 2023)	277.00	125.00	0.15	-
Ambilobe (Stolerie *et al.,* 2022)	120.00	58.00	0.18	0.50
Antsiranana II (Tsilailay *et al.,* 2026)	148.00	66.30	0.08	0.28
Antalaha (Ngoko *et al.,* 2025)	133.00	58.00	0.18	0.53

In contrast, a striking difference is observed with the neighboring district of Ambanja (Rahelivao *et al.,* 2023), where the average Ra_{eq} reaches 277 Bq·kg^{-1}, and the *AGDR* is 125 nGy.h^{-1}. This severe radiological anomaly in Ambanja is explained by the presence of alkaline complexes and carbonatites (Ampasindava peninsula) rich in rare earths, uranium, and thorium. The geology of Nosy-Be, although volcanic, is of a more common basaltic and rhyolitic nature, which justifies the absence of High Background Radiation Areas on the tourist island.

However, the modeling of the 50% occupancy factor highlights an issue frequently overlooked in global dosimetric studies: human behavior. While the soils of Nosy-Be are overall less radioactive than the global average, the prolonged time spent by Malagasy farmers in direct contact with the earth in crop fields compensates for this low radioactivity, raising the *ELCR* above the global average. This underscores the necessity of using demographic parameters adapted to developing countries when assessing risks.

IV. Conclusion

This study marks an important milestone by translating geochemical data concerning the natural radioactivity of Nosy-Be soils into actual public health risk evaluation parameters.

The results are largely reassuring. The main indicators, such as radium equivalent activity and the absorbed dose rate, are systematically below recommended limits. Nosy-Be soils can be used without restriction as building materials, and the level of ambient radiation poses no threat to the health of residents or tourists.

Nevertheless, the analysis reveals that an agricultural lifestyle, which implies a strong outdoor presence (50%), generates a long-term stochastic risk slightly higher than the global average, even though the annual dose remains well below recommended limits. The distribution of this risk, correlated with the recent volcanism in the western part of the island, provides an invaluable database for local authorities regarding radiation protection, land-use planning, and sustainable tourism development.

Acknowledgment

The authors are highly indebted to the Nuclear Techniques and Analysis at INSTN-Madagascar, as well as the Nuclear Metrology and Environment at the University of Antsiranana, for providing indispensable technical guidance and sustained partnership throughout the execution of this work.

References

[1] UNSCEAR. (2000). Sources and Effects of Ionizing Radiation, Vol. 1. United Nations Scientific Committee on the Effects of Atomic Radiation. Report to the General Assembly with Scientific Annexes. United Nations, New York.

[2] M. Tzortzis, H. Tsertos, S. Christofides, & G. Christodoulides. (2003). Gamma-ray measurements of naturally occurring radioactive samples from Cyprus, characteristic geological rocks. Radiation Measurements, 37(3), 221-229.

[3] European Commission, Joint Research Centre. (2019). European Atlas of Natural Radiation. Publication Office of the European Union, Luxembourg.

[4] H. C. Djaovagnono, Z. Donné, M. Rasolonirina, A. F. Solonjara, & B. Kall. (2025). Spatial Distribution of Natural Radioactivity from the ^{238}U and ^{232}Th Decay Series, and ^{40}K in the Volcanic Soils of Nosy-Be Island, Madagascar. International Journal of Scientific Engineering and Science, 9(7), 36-45.

[5] J. Beretka, & P. J. Mathew. (1985). Natural radioactivity of Australian building materials, industrial wastes and by-products. Health Physics, 48(1), 87-95.

[6] J. P. Stolerie, M. Rasolonirina, Z. Donné, N. Rabesiranana, & B. Kall. (2022). Distribution spatiale de la radioactivité naturelle du sol et leur impact dosimétrique sur la population du district d'Ambilobe, Madagascar. American Journal of Innovative Research and Applied Sciences, 15(3), 62-72.

[7] F. Ngoko, Z. Donné, F. R. Randrianantenaina, D. Rasolozafy, A. F. Solonjara, & B. Kall. (2025). Assessment of the Dosimetric Impact and Radiological Risk Associated with Natural Soil Radioactivity in the Antalaha District, Madagascar. International Journal of Scientific Engineering and Science, 9(4), 136-141.

[8] A. N. S. Tsilailay, Z. Donne, F. R. Randrianantenaina, A. F. Solonjara, & F. Asimanana. (2026). Radiological Risk Assessment for the Population of Antsiranana II District, Madagascar, due to External Exposure to Natural Radioactivity in Volcanic Soil. International Journal of Scientific Engineering and Science, 10(1), 146-151.

[9] J. E. Rahelivao, Z. Donné, A. Razafindrapata, A. I. Joelisoafara, M. Rasolonirina, & B. Kall. (2023). Study of Natural Radioactivity Levels and the Associated Radiological Hazards in Soil from Ambanja City and its Surroundings, Madagascar. International Journal of Innovative Research in Science, Engineering and Technology, 12(5), 4688-4698.

[10] ICRP. (2007). The 2007 Recommendations of the International Commission on Radiological Protection. ICRP Publication 103. Annals of the ICRP, 37(2-4), 1-332.

[11] B. F. Namq, Z. A. Hussein, S. Q. Othman, L. A. Najam, T. Y. Wais, M. I. Sayyed, H. Mansour, & U. Rilwan. (2025). Evaluation of radiological risks due to natural radionuclides in the soil of Khanaqin district, Diyala, Iraq. Physica Scripta, 100(1), 015310.

[12] E. O. Akuo-ko, F. Otoo, E. T. Glover, E. Amponsem, L. Tettey-Larbi, T. Ganbaatar, A. Csordás, A. Shahrokhi, & T. Kovács. (2025). Radiological Implications of Industrial Activities on Soil and Water: An Environmental Analytical Chemistry Perspective in Artisanal Gold-Mining Regions of Atiwa West. Applied Sciences, 15(1), 9857.

[13] G. D. Houndetoungan, O. H. Fachinan, M. B. Zinsou, S. B. M. G. Adjadohoun, G. Abogbo, G. Awede, M. Zoungrana, & K. M. Amoussou-Guenou. (2025). Evaluation of Public Exposure to Gamma Radiation in Cotonou, Southern Benin. Brazilian Journal of Radiation Sciences, 13(4), 01-24.

[14] M. J. Mvelase. (2026). Assessment of natural radioactivity and associated radiological health hazards in Mooifontein gold tailings. Discover Applied Sciences, (Article in Press).

[15] S. M. El-Bahi, A. Sroor, G. Y. Mohamed, & N. S. El-Gendy. (2017). Radiological impact of natural radioactivity in Egyptian phosphate rocks,

phosphogypsum and phosphate fertilizers. Applied Radiation and Isotopes, 123, 121-127.